

In vitro and *in vivo* assessment of biocompatibility of AZ31 alloy as biliary stents: a preclinical approach

Yong Song¹, Gaoping Qin¹, Lixue Du¹, Haitian Hu¹, Yong Han²

¹Department of Hepatobiliary Surgery, Shaanxi Provincial People's Hospital, Xi'an, Shaanxi, China

²Material Science and Engineering, Xi'an Jiaotong University, Beilin District, Xi'an, Shaanxi, China

Submitted: 28 March 2019; **Accepted:** 15 April 2019

Online publication: 31 January 2020

Arch Med Sci 2022; 18 (1): 195–205

DOI: <https://doi.org/10.5114/aoms.2020.92675>

Copyright © 2020 Termedia & Banach

Corresponding author:

Yong Song MD

Department of Hepatobiliary Surgery

Shaanxi Provincial People's Hospital

Xi'an, Shaanxi

China

E-mail: songyongbest@sina.com

Abstract

Introduction: Biomaterial technology due to its lack of or minimal side effects in tissues has great potential. Traditionally biomaterials used were cobalt-chromium, stainless steel and nitinol alloys. Biomaterials such as magnesium (Mg) and zinc (Zn) have good biocompatibility and consequently can be a potential material for medical implants. To date, the effects of AZ31 alloy stent on cell apoptosis are still unclear. The current investigation was designed to determine the effect of AZ31 alloy stent on necrosis and apoptosis of common bile duct (CBD) epithelial cells.

Material and methods: We experimented with application of different concentrations of AZ31 alloy stent to primary mouse extrahepatic bile epithelial cells (MEBECs) and estimated the effect on apoptosis and necrotic cells. Apoptosis and pro-apoptosis expression were estimated through real-time PCR. For *in vivo* protocol, we used rabbits, implanted the AZ31 bile stent, and estimated its effect on the CBD. AZ31 (40%) concentration showed an effect on the apoptotic and necrotic cells.

Results: Real-time PCR revealed that AZ31 (40%) concentration increased the apoptotic genes such as NF- κ B, caspase-3, Bax and Bax/Bcl-2 ratio as compared to the control group. In the *in vivo* experiment, AZ31 alloy stents were implanted into the CBD and showed an effect on the alteration the hematological, hepatic and non-hepatic parameters.

Conclusions: To conclude, it can be stated that AZ31 induces apoptosis via alteration in genes including nuclear factor kappa-B (NF- κ B), caspase-3, Bax and Bax/Bcl-2 ratio and improved the hematological, hepatic and non-hepatic parameters.

Key words: biodegradable stent, AZ31, apoptosis, common bile duct.

Introduction

Common bile duct (CBD) disease presents a momentous risk to the patient, since it may lead to biliary colic, pancreatitis or cholangitis and obstructive jaundice. Traditionally, surgeons used T-tube drainage for removal of CBD lesion or stones. Several researchers suggest that a T-tube drainage system allows the edema or spasm of the sphincter with the trauma of exploration. Despite the advantage of the T-tube, several disadvantages are associated with it, including bile leakage and CBD obstruction seen after CBD surgery. Common bile duct surgery by T-tube requires the patient to be under constant observation with restric-

tion of food habit. There is always a high chance of infection after CBD treatment, especially when the T-tube is removed, a reason for more risk to the patient. For avoidance of T-tube complications, the surgeons and researchers now focus on an alternative to treat CBD.

Day by day, biomaterial technology is gaining more popularity due to the lack of adverse reaction in and on the tissue. Biodegradable implant material has the advantage that it can easily be absorbed, gradually dissolved, and there is no need for surgical removal after surgery. Traditional metallic materials such as cobalt-chromium, stainless steel and nitinol alloys have been commonly used in biomaterial technology [1]. Biomaterial such as magnesium (Mg) and zinc (Zn) both have good biocompatibility and consequently make good potential material for medical implants [2]. Biodegradable Mg alloy has more potential due to its excellent mechanical properties and good biocompatibility with the tissues [3]. Nowadays magnesium based biomaterial has been most commonly used as a biodegradable medical implant device due to excellent mechanical properties [4, 5].

The flow rate plays an important role during biodegradation of Mg and its alloys. The various investigations reported that reduced flow rate compositions may result in excellent corrosion resistance in a bare mate, involving the application in other non-vascular fluid conditions [6–8]. On the basis of the above facts, the researchers focused their research mainly on Mg and its alloy (non-vascular endoluminal stents). Pure Mg has a corrosion rate of 0.01594 ml/cm²/h for 10 days mainly in the esophageal stent. Another report suggests that Mg has a relaxing factor in airway smooth muscles of rabbits. One study on a stent (Mg-3Y) implanted into the trachea of a canine rodent model showed no adverse effect found in the structure of adjacent cartilage after 8 weeks [4, 5, 7, 9]. JDBM alloy was implanted for 1–2 years as a tracheal stent in rodent (rabbits) and induced tracheomalacia via coating the multiple layers. Also, Mg-based alloys used as an intestinal stent have exhibited a significantly higher apoptosis rate when implement as intestinal epithelial cells. *In vitro* investigation of AZ31 stent used in an artificial urine system has shown good antibacterial activity and it is used as a ureteral stent [4, 9].

It is necessary to keep supporting material in the CBD to protect it from post-operative CBD stenosis. This has led to adverse immunological and inflammatory responses [10, 11]. These reactions commonly trigger apoptosis necessary to remove the inflamed and damaged tissue and maintain the regeneration and healing mechanisms [11, 12]. Necrosis is generally induced by cell poison effects and apoptosis showed the effect on the cell

biological and morphological features. Apoptosis plays a defensive role in immune reaction or cell damage via noxious or disease agents [10–12]. Dissimilar to apoptosis, the proteolytic enzyme (cytoplasmic content) of secretion of necrotic cells enters into the surrounding tissue and induces the inflammation. Necrosis frequently arises in pathological changes, whereas apoptosis is a normal physiological event [13–15].

Materials such as titanium, polymer and silicone rubber are most commonly employed as CBD supporting systems. Silicon rubber stent (T-tube) can cause complications such as dehydration, biliary fistula, and incapability to clean the drain tube in CBD [16, 17]. Another stent such as polymeric and titanium alloy can induce the accumulation of bacteria, epithelial hyperplasia, and bio-film sludge that need to be eliminated. Due to the limitation of the above-discussed stent, different types of biodegradable CBD stent have been intended to replace the non-degradable stents [18, 19]. The biodegradable stent has the advantage in cleaning, reduction in deposition of biofilm with size alteration. Several types of research suggest that magnesium alloy is the best biodegradable implanting material for its biocompatibility and excellent mechanical property. Magnesium alloy stents are mostly used in surgical clips, vascular stents, bone implants, surgical sutures, and staples.

There are limitations for the animal experimental studies, as they are often used in big animals such as dogs or pigs (usually they use 4–6 animals). A big animal has two disadvantages: first, they are too expensive and limit animal use in the study, and second they have a limited number of antibodies against the big animals, which adds a more difficult molecular experiment in CBD. In the current investigation, we tried to explore the effect of AZ31 alloy on necrosis or apoptosis via *in vitro* and *in vivo* experimental studies. Primary mouse extrahepatic bile epithelial cells (MEBECs) were able to show a concentration base effect of AZ31 alloy stent to investigate the apoptotic gene expression such as tumor necrosis factor- α (TNF- α), B-cell lymphoma 2 (Bcl-2), Bax, NF- κ B and caspase-3. Further, we investigated the long term effect of AZ31 alloy stent on different biochemical, hematological and non-hepatic parameters.

Material and methods

Material and extract preparation

Biodegradable stent AZ31 tubes were prepared as extruded AZ31 alloy, with purity of Zn 99.999% and Mg 99.99%. The composition of AZ31 alloy is presented in Table I.

Table I. Chemical composition of AZ31 alloys bile duct stent and composition of AZ31 stent

Material	Chemical compositions (wt%)					
	Al	Zn	Mn	Si	Fe	Ca
AZ31	3.1	0.73	0.25	0.02	0.005	0.0014
No.	Sample	pH	Osmolality	Mg ²⁺ concentration		
1	Control	7.20 ±0.11	254.1 ±1.8	11.2		
2	20%	7.34 ±0.15	276.0 ±1.9	89.2 ±30.2		
3	40%	7.69 ±0.23	292.0 ±2.1	176.3 ±35.6		
4	80%	7.83 ±0.12	343.4 ±3.4	389.4 ±40.4		
5	100%	8.11 ±0.18	378.3 ±2.8	779.0 ±120.0		

A high purity crucible with high temperature (700–750°C) was used for the preparation of AZ31 alloy in the muffle furnace. After 30 min, temperature 700°C, metal was melted and transferred into the steel mold at a high temperature. Cover gas such as argon (99.99% purity) was employed throughout the casting and melting processes. The solid solution of AZ31 alloy treated at 350°C for 120 min followed by water treatment. Finally, the hot treated alloy sample was hot extruded at 250°C at an extrusion ratio (8 : 2). Finally, the AZ31 was placed into tube-shaped samples for experimental study. Tube shaped samples of AZ31, with dimensions of 1.0 mm (luminal diameter), 0.1 mm (thickness) and 5 mm (length), were used throughout the experiment. In a prior experimental study, all the tubes were polished with hydrochloric acid (2 ml), glycerol (20 ml), acetic acid (5 ml) and nitric acid (3 ml) and washed with distilled water and ethanol. Subsequently, the tubes were re-sterilized and weighed [20, 21].

In vitro model

Briefly, modified Dulbecco’s Eagle’s medium (DMEM) suspended into glycerine and fetal bovine serum was used as extraction medium. The extraction medium (1.25 cm²/ml) and the immersed sample (AZ31) were kept in a humidified area (CO₂ 5%) at 37°C for 1 day. After that, the extraction medium was collected and the supernatant was successfully removed, and centrifuged and stored at 4°C in a refrigerator.

For observing the concentration-dependently effect, the extract was serially diluted (100–20) with DMEM. We used inductively coupled plasma-atomic emission spectroscopy (ICP-AES) for the determination of the concentration of released Zn and Mg ions in the AZ31 alloy extract [22].

Surgery

New Zealand rabbits (3.0 ±0.5 kg) were used in our animal study with approval from the institu-

tional ethical committee. The rabbits were kept in a single cage and received the standard diet and water *ad libitum*.

Animals were fasted overnight (10 h) before surgery. Rabbits were anesthetized by iv injection of sodium pentobarbital (30 mg/kg, b.w.). The epigastrium tissue was cut (layer by layer), the gastrointestinal tract (GI tract) was pushed and the duodenum was picked up to locate the common bile duct, with the expanded connection of the duodenum and common bile duct visible. A bile duct stent (AZ31) was placed in the common bile duct through an angle incision (2 mm) at the anterior wall of the bile duct. The incision and epigastrium were sealed by suture followed by 5 days of intramuscular injection of penicillin. After the surgery, the rabbits were sacrificed at a regular time interval for analysis of different biochemical and hematological parameters [23–25].

Cell apoptosis

Cell apoptosis was detected by kit as per the manufacturer’s instruction. Briefly, AZ31 alloy with different concentrations (40–100%) was treated with MEBDEC’s cultured cells along with the control group. Trypsin (0.25%) was added for recovery cells and recovered cells were re-suspended in buffer (Annexin-binding Buffer). After 15 min Annexin-binding Buffer was added, samples were kept in an ice-cold water bath and estimation was made through fluorescence emission at 530 nm [26, 27].

mRNA isolation and quantification

AZ31 alloy with concentration 40–100% treated with MEBDEC’s cultured cells along with a control group and Trizol reagent was used to determine the quantity and concentration of ribonucleic acid (RNA). Briefly, primers presented in Table II were designed and synthesized and real-time polymerase chain reaction (PCR) was used for estimation of mRNA quantity [28, 29].

Table II. Primer for real time PCR

No.	Gene	Primer sequence	
		Reverse	Forward
1	Bax	GCCCCAGTTGAAGTTGCCATCAG	GCGAGTGTCTCCGGCGAATT
2	B-actin	ACTCCTGCTTGCTGATCCACATCT	TTGCTGACAGGATGCAGAAGGAGA
3	Bcl-2	AATCAAACAGAGGTGCGATGCTGG	TTGTGGCCTTCTTTGAGTTCGGTG
4	NF-κB	CCGTGGGGCATTTTGTTTCAG	CCACGAGGCAGCACATAGAT
5	TNF-α	CCGGACTCCGCAAAGTCTAA	ACCGTCAGCCGATTGCTAT
6	Caspase-3	CCGTACCAGAGCGAGATGAC	GAGCTTGAACGGTACGCTA

Hematological profile

Hematological parameters white blood cells (WBC), hemoglobin (Hb) and platelets were estimated via using the standard kits as per the manufacturer’s instructions (Sigma Aldrich, USA).

Hepatic parameters

Hepatic parameters such as alanine aminotransferase (ALT) and aspartate aminotransferase (AST) were estimated through standard kits as per the manufacturer’s instructions (Sigma Aldrich, USA).

Non-hepatic parameters

Non-hepatic parameters such as creatinine, urea nitrogen and total bilirubin estimated via using the standard kits as per manufacturer instructions (Sigma Aldrich, USA).

Statistical analysis

Statistical analysis was performed with the GraphPad Prism software package (USA). The experimental values were analyzed using paired sample tests and presented as the mean ± standard deviation. One-way analysis of vari-

ance was performed to evaluate differences between groups. The Dennett test was used when equal variances were not assumed. $P < 0.05$ was considered to indicate a statistically significant difference.

Result

Effect on apoptosis

Figure 1 exhibits the fluorescence intensity of AZ31 extracts. The cells are divided into 3 distinct quadrants. The first quadrant (left) demonstrated the normal visible cells and the 2nd quadrant (lower) illustrated the apoptotic cells and the 3rd quadrant exhibited the necrotic and apoptotic/necrotic cells (data not shown). Dose-dependent treatment of AZ31 extract exhibited an effect on the apoptotic and necrotic cells. On day 1, AZ31(80%) extract concentration showed a larger apoptotic effect and the same results were observed in the necrotic cells treated with AZ31 (80%) (Figure 1). After 1 day, AZ31 (100%) showed significantly ($p < 0.05$) less Bax mRNA expression than the other groups. On day 3, the mRNA expression of Bax was significantly ($p < 0.05$) increased in AZ31 (40%) extract compared to other groups. On the other hand, no difference was observed in the Bcl-2 mRNA expression in the AZ31 (40, 80 and 100%) and control group.

Figure 2 demonstrates the ratio of Bax to Bcl-2 with more accuracy and reflects the cell sensitivity to apoptotic stimuli than the individual expression of these two genes. AZ31 (40%) extract treated with MEBECs for 72 h – this group has a higher level of Bax/Bcl-2 ratio as compared to other groups.

Figure 3 displays the relative mRNA expression of TNF-α, caspase-3 and NF-κB of cultured MEBECs. There was no significant difference between extract groups and control group on day 1 in expression of NF-κB. After day 3, the 40% extract group showed a higher expression level of NF-κB in comparison to the control group. In the case of TNF-α mRNA expression, no significant differences were observed between extract groups and the control group on

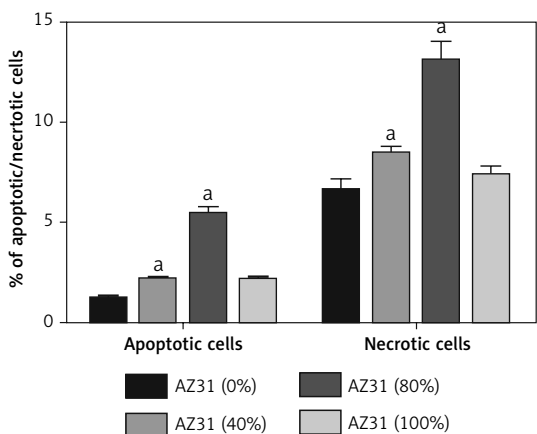


Figure 1. Percentage of apoptotic cells and necrotic cells when mouse extrahepatic bile epithelial cells are cultured in the extraction media

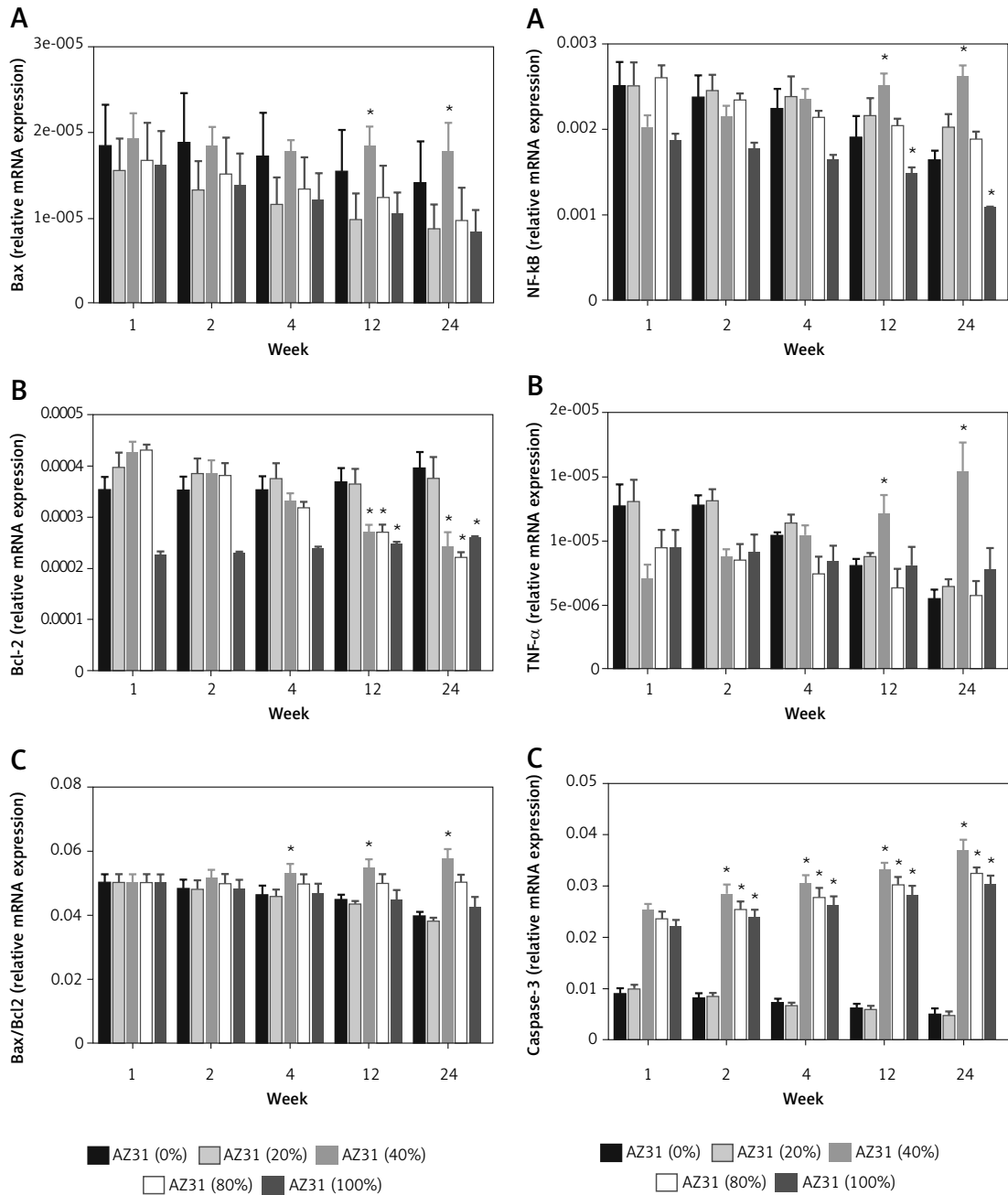


Figure 2. Effect on relative mRNA expression. **A** – Bax, **B** – Bcl-2 and **C** – Bax/Bcl-2 when mouse extrahepatic bile epithelial cells are cultured in media for a period of 1 and 3 days

Figure 3. Effect on the relative mRNA expression. **A** – NF-κB, **B** – TNF-α and **C** – caspase-3 when mouse extrahepatic bile epithelial cells are cultured in media for a period of 1 and 3 days

both day 1 and day 3. The expression of caspase-3 on day 1 was higher in 80 and 100% extracts than in the control group, and after day 3 all the experiment groups exhibited increased activity in caspase-3 expression as compared to the control group.

Effect on apoptotic and pro-apoptotic gene expression

Figure 2 exhibits the effect of AZ31 extract on apoptotic gene expression at different time inter-

vals. Figure 3 A shows the effect of AZ31 extract on Bax gene expression at a different time intervals. Week 1 showed almost the same level of Bax in all concentrations of AZ31 (0%, 20%, 40%, 80% and 100%). As time increases, the relative expression of Bax changes in all concentration groups, AZ31 (40%) showed the increased relative gene expression of Bax at the end of the experimental study. A similar pattern was observed in the Bcl-2 relative gene expression. AZ31 (40%) showed the enhanced expression of Bcl-2 as compared to other

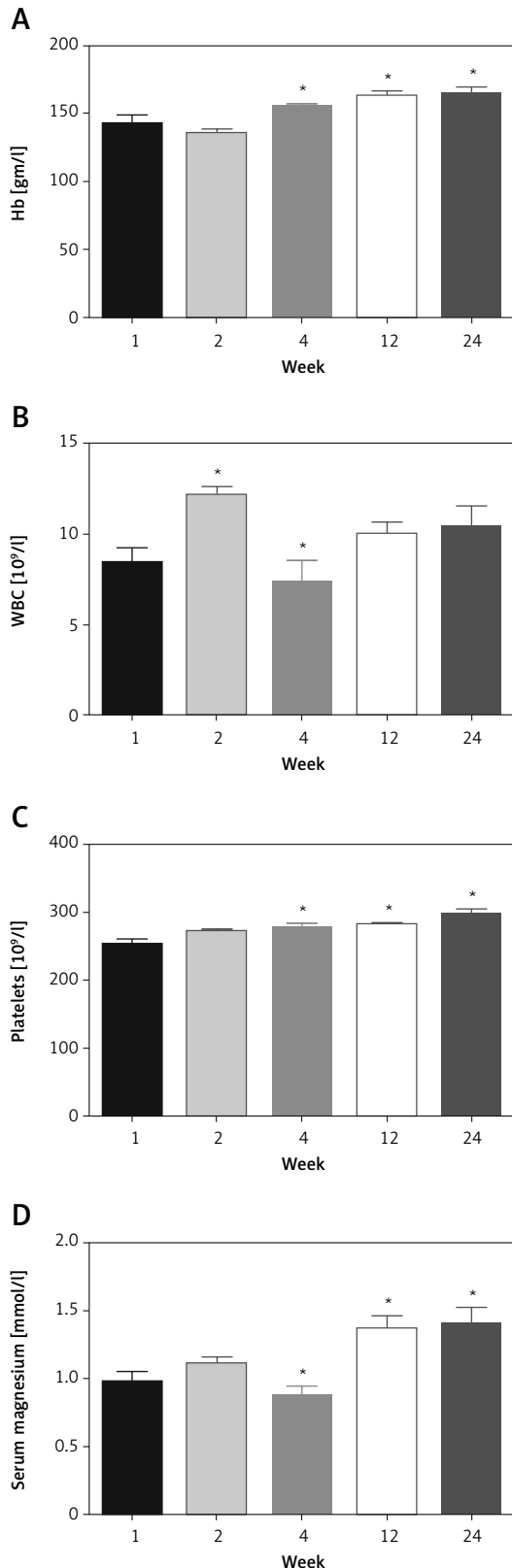


Figure 4. Effect on the hematological profile. **A** – hemoglobin (Hb), **B** – white blood vells (WBC), **C** – platelets and **D** – serum magnesium. There is a significant difference compared with data gathered before surgery ($p < 0.05$)

groups (Figure 2 B). Figure 3 C illustrated the relative expression of Bax/Bcl-2 in AZ31 extract treatment. AZ31 (40%) extract showed increased expression.

Figure 3 A shows the effect of different concentrations of AZ31 extracts on the NF- κ B expression. AZ31 (40%) showed down-regulation of NF- κ B expression. A similar trend was observed in TNF- α and caspase-3; the expression of TNF- α and caspase-3 decreased in the AZ31 (40%) treated group.

Effect of AZ31 on hematological parameters

Figure 4 showed the effect of AZ31 stent on the hematological parameters. Hemoglobin level was significantly ($p < 0.05$) increased during the first week and was reduced the next week. After that, the hemoglobin level significantly ($p < 0.05$) increased in the next week and continued to increase until the last week of the experimental study (Figure 4 A). Figure 4 B demonstrates the WBC effect; initially, WBC content increased and in the next week the level was boosted and after that, the level of WBC was normal at the end of the experimental study. Figure 4 C demonstrates that the platelet count increased from the first week and remained enhanced until the end of the experimental study. Figure 4 D illustrated the serum magnesium concentration and data showed that the level of Mg²⁺ significantly ($p < 0.05$) decreased in first 2 weeks and after that, it remained at a normal level as compared to the initial level.

Effect of AZ31 on hepatic parameters

Figure 5 A shows the ALT level its level slightly reduced in the first 12 weeks but after that, the level of ALT increased (week 24). An opposite trend was observed in the AST, the AST level was increased in the 1 to 4 week and after that the level of AST going to reduced and reached to the normal level.

Effect of AZ31 on non-hepatic parameters

Figure 6 exhibited the effect AZ31 on non-hepatic parameters. According to Figure 6 at the creatinine level was unaltered by the AZ31 stent until the end of the experimental study. Figure 6 B exhibits the content of urea nitrogen; urea nitrogen level was significantly ($p < 0.05$) decreased in the first week and in the next week the level of urea nitrogen increased and reached almost the initial level at end of the experimental study. Figure 6 C demonstrates the total bilirubin; the level of bilirubin significantly ($p < 0.05$) increased at the start of the week (week 4) and after that the content

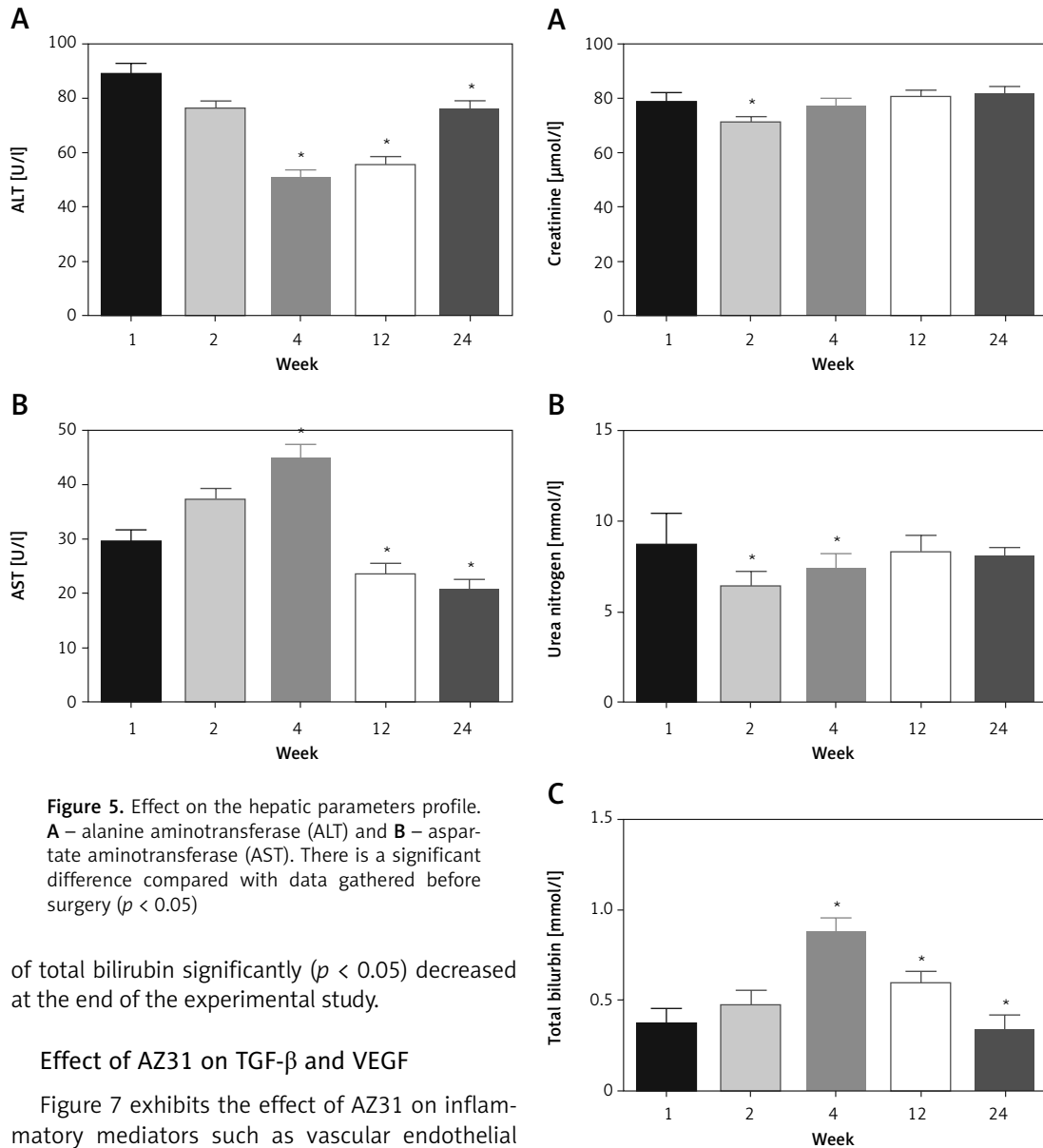


Figure 5. Effect on the hepatic parameters profile. **A** – alanine aminotransferase (ALT) and **B** – aspartate aminotransferase (AST). There is a significant difference compared with data gathered before surgery ($p < 0.05$)

of total bilirubin significantly ($p < 0.05$) decreased at the end of the experimental study.

Effect of AZ31 on TGF- β and VEGF

Figure 7 exhibits the effect of AZ31 on inflammatory mediators such as vascular endothelial growth factor (VEGF) and transforming growth factor β (TGF- β). The level of TGF- β decreased in the first week to the fourth week and recovered in the last 24 weeks. A similar result was observed in the case of VEGF level.

Effect of AZ31 on apoptosis

Figure 8 represents the experiment on BAX, Bcl-2 and BAX/Bcl-2 levels. In the first 2 weeks, the levels of BAX, Bcl-2 and BAX/Bcl-2 were decreased and after that, the levels of BAX, Bcl-2 and BAX/Bcl-2 increased until 24 weeks.

Discussion

Following CBD examination, the T-tube was inserted in the CBD to provide support and maintain the open CBD. Conversely, the treatment cost is higher due to a prolonged stay in the hospital.

Figure 6. Effect on the non-hepatic parameters profile. **A** – Creatinine, **B** – total urea nitrogen and **C** – bilirubin. There is a significant difference compared with data gathered before surgery ($p < 0.05$)

Another fact is the risk of T-tube placement, such as increased mortality or morbidity and increased biliary infection, migration of the T-tube inducing the bile duct obstacle, peritonitis, bile leakage following the removal of the T-tube [30]. Now the researchers and surgeons focus on the new therapy for the CBD and the choice of the researchers and surgeons is a biodegradable stent. The advantage of a biodegradable stent is that it is easy to implant, prolong the duration of action, and there is no need for surgery to remove it from the body. Biomaterial technology is an emerging topic due to clinical use with less or no adverse effect. Mag-

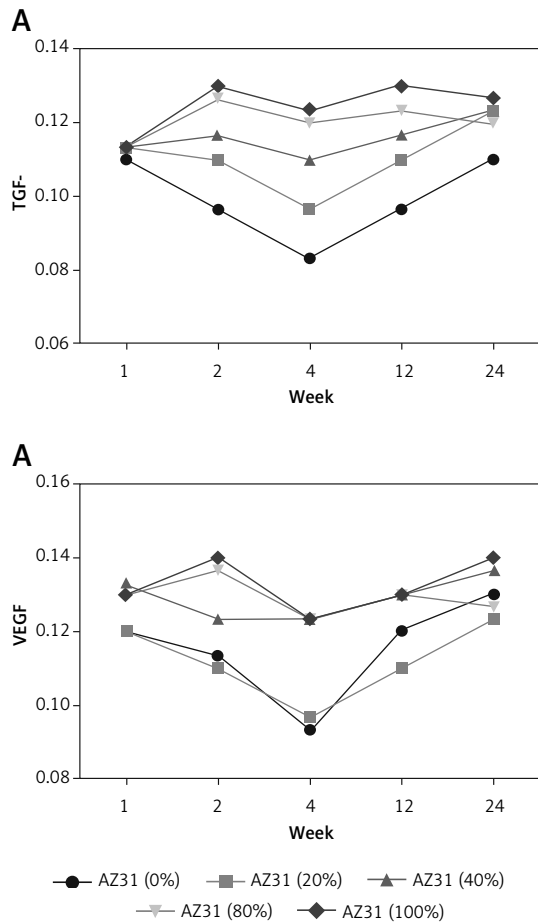


Figure 7. Effect on the transforming growth factor β (TGF- β) (A) and vascular endothelial growth factor (VEGF) (B) expression

nesium and aluminum are both metals having excellent biocompatibility with tissues or organs and due to this property they are widely used for medical implants. Due to the high demand of bimetallic magnesium and aluminum, they are widely used in various clinical therapies [31]. Various previously published literature suggest that the biomaterial might persuade the monocytes, inflammation reaction, phagocytosis and macrophages migration [16, 32]. Consequently, it should be taken into consideration that excessive deposition of degradation products due to excessive loading of burst release or organism regulation would in turn depreciate the local physical condition [33–35]. In the current investigation, we scrutinized the long term effect of biomaterial stent (AZ31) in the common bile duct. Before implanting the stent into the tissue, the medical professional mainly focuses on the safety issue. Before we start the experimental study, we take the safe combination of bimetal which is presented in Table I. We used the AZ31 alloy stents with 1.0 mm diameter, length 5 mm and thickness 0.1 mm which were

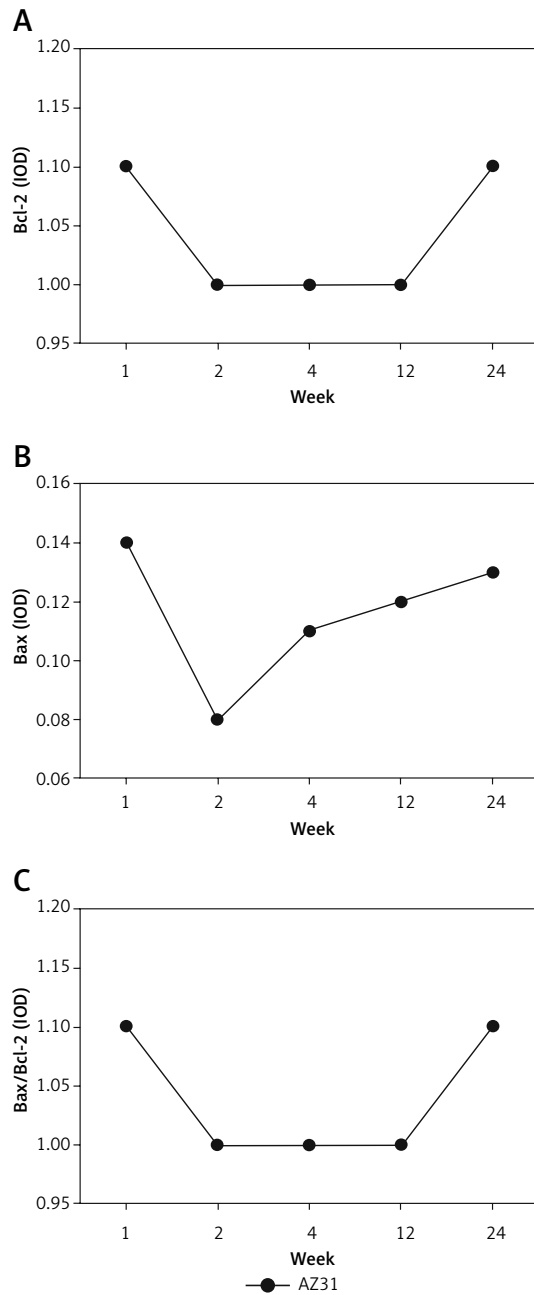


Figure 8. Immunohistochemical staining of Bcl-2 and Bax: A – the Bcl-2 expression, B – the Bax expression, C – the ratio of Bax/Bcl-2 expression

implanted into the rabbits and were screened at regular time intervals using CT scanning. On scanning, the stents degraded in the first week (~67%), second week (~38%), fourth week (~24%), twelfth week (~16%) and finally completely degraded at twenty weeks after the surgery. In the current study, we observed the effect of AZ31 stent on hematological, hepatic, non-hepatic parameters and apoptosis parameters.

The term apoptosis was firstly used by Kerr Wylie (non-classic paper) and Currie to define the mor-

phological as discrete from the cell death [36, 37]. Another apoptosis is defined as having a preventive effect viz., exclusion of unwanted cells and upholds the host stability [36, 37]. The mechanism of apoptosis involved in the process of transpired the mammalian cells from cell death occurred during the expansion of nematode. *In vitro* investigations suggest that AZ31 alloy stent extract boosts MEBECs apoptosis via using the low concentration and on the contrary AZ31 alloy stent extract significantly enhanced the necrosis/apoptotic necrosis in a concentration-dependent manner [38, 39]. 80% concentration of AZ31 alloy stent extract exhibited considerably higher apoptosis of MEBECs cultured as compared to other treatment. When the concentration reached 100% the apoptotic and necrosis/apoptotic necrosis level enhanced and supported the apoptosis. Conversely, the result exhibited that no difference was observed in between the apoptotic necrosis and necrotic cells. In long culture treatment, apoptotic cells will undergo secondary necrosis, which is called late apoptosis or post-apoptotic necrosis [40]. In the current experimental study, after the cultures, the cells were found as necrotic and further converted into the secondary necrosis. As a result, our experimental result showed that the necrosis may be affected via late apoptosis or post-apoptotic necrosis.

Bax is a pro-apoptotic protein [41] and Bcl-2 is an anti-apoptotic protein [42] and these are discovered to be mammalian cell death regulators [43, 44]. The researchers suggest that the Bcl-2 protein is involved in the negative and positive regulation of apoptotic cell death [43, 44]. Bcl-2 (anti-apoptotic members) regulates the negative cell death and protects the cells from undergoing apoptosis induced via numerous stimuli of various cells [45]. On the other hand, pro-apoptotic proteins such as Bax accelerate or boost cell death [46, 47]. *In vitro* studies demonstrated that after 1 week the Bax and Bax/Bcl-2 mRNA expression was significantly higher in 40% of extracts and remained higher until 24 weeks. On the basis of the results, we can say that 40% of AZ31 alloy stent extract induced the apoptosis in MEBEGs in an *in vitro* atmosphere [47, 48].

In the *in vivo* experimental study, AZ31 alloy extract did not exhibit any significant difference in the apoptosis relative genes. Therefore at 1-week post-operation, the AZ31 alloy group exhibited higher Bax expression as compared to the control group and no significant difference was observed in the Bax/Bcl-2 ratio in the AZ31 alloy and control group. The apoptosis mechanism is very complex. Several apoptosis mediators such as caspase-3, TNF- α and NF- κ B play an important role in the apoptosis mechanism [49, 50]. The apoptosis mediators are activated via transactivating gene expres-

sion of anti-apoptosis [51–54]. Several researchers suggest that the NF- κ B pathway is a crucial factor in the cell reaction to apoptotic stimuli [55–57]. During the NF- κ B pathway, TNF- α (downstream protein) can start the apoptosis reaction via cross-link protein or ligand binding. Our experimental study suggests the alteration of the NF- κ B concentration-dependent manner of AZ31. AZ31 alloy extract (40%) showed significantly increased expression of NF- κ B at a regular time interval. A similar result was observed in the TNF- α concentration; AZ31 alloy extract (40%) demonstrated increased expression [52–54, 58]. Another apoptosis parameter, caspase-3, is considered as a significant marker of inflammation and plays an important role in the apoptosis pathway [57]. In our experimental study, caspase-3 expression was more sensitive to changes in the AZ31 alloy concentration. The data revealed that the expression of caspase-3 was significantly increased in AZ31 alloy extract (40%, 80% and 100%) treatment. In short, we have found that AZ31 alloy extract (40%) boosted the apoptosis relative genes such as Bax, Bax/Bcl-2 ratio and critical apoptotic protein viz., caspase-3 and NF- κ B. In the current experimental investigation, AZ31 alloy extract (40%) could induce the alteration in the apoptosis genes in both intestinal epithelial cells and intestinal tract tissues. On the basis of the result, we can say that aluminum plays an important role in the activation of NF- κ B expression [59–61].

In conclusion, collectively, we can say that the advancement of the stent reduces the risk of infection. In the current experimental study, *in vitro* and the *in vivo* study was performed to scrutinize the biocompatibility of AZ31 with CBD. Our study suggests that the AZ31 stent gradually degraded in the CBD in the rabbits. AZ31 stent does not influence the biochemical parameters. The reduced level of VEGF expression may be related to lowering the stimulation resulting from the degradation of AZ31 alloy. Thus, it can be concluded that the AZ31 alloy stent is a safe biocompatible material for CBD.

Acknowledgments

The authors are very thankful to the natural science foundation of Xi'an city science and Technology Department, China Postdoctoral Science Foundation, Chinese medicine in Shaanxi Province Administration of traditional Chinese medicine scientific Postdoctoral Science Foundation and the natural science foundation of Shanxi Provincial science and Technology Department.

The authors are very thankful to natural science foundation of Xi'an city science and Technology Department (Project Number: 2012D37), China Postdoctoral Science Foundation (Project

Number: 2014M552459), Chinese medicine in Shaanxi Province Administration of traditional Chinese medicine scientific Postdoctoral Science Foundation (Project Number: JCPT029) and the natural science foundation of Shanxi Provincial science and Technology Department (Project Number: 2017JM8138) for providing the funding for the current study.

Conflict of interest

The authors declare no conflict of interest.

References

1. Chen Y, Yan J, Zhao C, et al. In vitro and in vivo assessment of the biocompatibility of an Mg-6Zn(n) alloy in the bile. *J Mater Sci Mater Med* 2014; 25: 471-80.
2. Liu L, Li N, Lei T, Li K, Zhang Y. The in vitro biological properties of Mg-Zn-Sr alloy and superiority for preparation of biodegradable intestinal anastomosis rings. *Med Sci Monit* 2014; 20: 1056-66.
3. Legeais JM, Werner I, Briat B, et al. A new biomaterial for intraocular lens. Experimental in vivo study. *Vision Res* 1995; 35: Suppl 1: S125.
4. Witte F, Hort N, Vogt C, et al. Degradable biomaterials based on magnesium corrosion. *Current Opinion in Solid State and Materials Science* 2008; 12: 63-72.
5. Walker J, Shadanbaz S, TBF Woodfield, Staiger MP, Dias GJ. Magnesium biomaterials for orthopedic application: a review from a biological perspective. *J Biomed Mater Res B Appl Biomater* 2014; 102: 1316-31.
6. Oosterbeek RN, Seal ChK, Seitz JM, Hyland MM. Polymer-bioceramic composite coatings on magnesium for biomaterial applications. *Surface and Coatings Technology* 2013; 236: 420-8.
7. Mueller WD, Lucia Nascimento M, Lorenzo de Mele MF. Critical discussion of the results from different corrosion studies of Mg and Mg alloys for biomaterial applications. *Acta Biomater* 2010; 6: 1749-55.
8. Peng Q, Li K, Han Z, et al. Degradable magnesium-based implant materials with anti-inflammatory activity. *J Biomed Mater Res A* 2013; 101: 1898-906.
9. Witte F. Reprint of: The history of biodegradable magnesium implants: a review. *Acta Biomater* 2015; 23 Suppl: S28-40.
10. Buddingh KT, Nieuwenhuijs VB, van Buuren L, Hulscher JB, de Jong JS, van Dam GM. Intraoperative assessment of biliary anatomy for prevention of bile duct injury: a review of current and future patient safety interventions. *Surg Endosc* 2011; 25: 2449-61.
11. Gonzalez FJ, Dominguez E, Lede A, Jose P, Miguel P. Migration of vessel clip into the common bile duct and late formation of choledocholithiasis after laparoscopic cholecystectomy. *Am J Surg* 2011; 202: e41-3.
12. Dziri C, Haouet K, Fingerhut A, Zaouche A. Management of cystic echinococcosis complications and dissemination: Where is the evidence? *World J Surg* 2009; 33: 1266-73.
13. Manzato E, Fellin R, Baggio G, Walch S, Neubeck W, Seidel D. Formation of lipoprotein-X. Its relationship to bile compounds. *J Clin Invest* 1976; 57: 1248-60.
14. Yasui T, Takahata S, Kono H, et al. Is cholecystectomy necessary after endoscopic treatment of bile duct stones in patients older than 80 years of age? *J Gastroenterol* 2012; 47: 65-70.
15. Diao M, Li L, Cheng W. Is it necessary to ligate distal common bile duct stumps after excising choledochal cysts? *Pediatr Surg Int* 2011; 27: 829-32.
16. Williams EJ, Green J, Beckingham I, Parks R, Martin D, Lombard M; British Society of Gastroenterology. Guidelines on the management of common bile duct stones (CBDS). *Gut* 2008; 57: 1004-21.
17. Wang GJ, Gao CF, Wei D, Wang C, Ding SQ. Acute pancreatitis: etiology and common pathogenesis. *World J Gastroenterol* 2009; 15: 1427-30.
18. Verbesev JE, Birkett DH. Common bile duct exploration for choledocholithiasis. *Surg Clin North Am* 2008; 88: 1315-28.
19. Haney JC, Pappas TN. Management of common bile duct injuries. *Oper Tech General Surg* 2008; 175-84.
20. Morisada Y, Fujii H, Nagaoka T, Fukusumi M. MWCNTs/AZ31 surface composites fabricated by friction stir processing. *Materials Science and Engineering: A* 2006; 419: 344-8.
21. Henderson SE, Verdalis K, Maiti S, et al. Magnesium alloys as a biomaterial for degradable craniofacial screws. *Acta Biomater* 2014; 10: 2323-32.
22. Chen Y, Yan J, Wang X, et al. In vivo and in vitro evaluation of effects of Mg-6Zn alloy on apoptosis of common bile duct epithelial cell. *Biomaterials* 2014; 27: 1217-30.
23. Xue D, Yun Y, Tan Z, Dong Z, Schulz MJ. In vivo and in vitro degradation behavior of magnesium alloys as biomaterials. *J Materials Sci Technol* 2012; 28: 261-7.
24. Huan ZG, Leeflang MA, Zhou J, Fratila-Apachitei LE, Duszczyn J. In vitro degradation behavior and cytocompatibility of Mg-Zn-Zr alloys. *J Mater Sci Mater Med* 2010; 21: 2623-35.
25. Bergsma JE, Rozema FR, Bos RR, Boering G, de Bruijn WC, Pennings AJ. In vivo degradation and biocompatibility study of in vitro pre-degraded as-polymerized polylactide particles. *Biomaterials* 1995; 16: 267-74.
26. Luu NT, Rainger GE, Nash GB. Kinetics of the different steps during neutrophil migration through cultured endothelial monolayers treated with tumour necrosis factor-alpha. *J Vasc Res* 1999; 36: 477-85.
27. Kim HS, Luo L, Pflugfelder SC, Li DQ. Doxycycline inhibits TGF- β 1-induced MMP-9 via Smad and MAPK pathways in human corneal epithelial cells. *Invest Ophthalmol Vis Sci* 2005; 46: 840-8.
28. Fang Y, Chen Y, Yu L, et al. Inhibition of breast cancer metastases by a novel inhibitor of TGF β receptor 1. *J Natl Cancer Inst* 2013; 105: 47-58.
29. Zhuo Z, Zhang L, Mu Q, et al. The effect of combination treatment with docosahexaenoic acid and 5-fluorouracil on the mRNA expression of apoptosis-related genes, including the novel gene BCL2L12, in gastric cancer cells. *In Vitro Cell Dev Biol Anim* 2009; 45: 69-74.
30. Banas T, Pitynski K, Okon K, et al. Immunoexpression of DNA fragmentation factor 40, DNA fragmentation factor 45, and B-cell lymphoma 2 protein in normal human endometrium and uterine myometrium depends on menstrual cycle phase and menopausal status. *Arch Med Sci* 2018; 14: 1254-62.
31. Sukhikh GT, Malaitsev VV, Bogdanova IM. Application potential of human fetal stem/progenitor cells in cell therapy. *Bull Exp Biol Med* 2008; 145: 114-21.
32. Tazuma S. Gallstone disease: epidemiology, pathogenesis, and classification of biliary stones (common bile duct and intrahepatic). *Best Pract Res Clin Gastroenterol* 2006; 20: 1075-83.
33. Fukumura Y, Nakanuma Y, Cong H, Hara K, Kakuda Y, Nakanuma Y. Intraductal papillary neoplasm of the bile

- duct. In: Pathology of the Bile Duct. Nakanuma Y (ed.). Springer 2017.
34. Chan DS, Jain PA, Khalifa A, Hughes R, Baker AL. Laparoscopic common bile duct exploration. *Br J Surg* 2014; 101: 1448-52.
 35. Lyass S, Phillips EH. Laparoscopic transcystic duct common bile duct exploration. *Surg Endosc* 2006; 20 Suppl 2: S441-5.
 36. Zeiss CJ. The apoptosis-necrosis continuum: insights from genetically altered mice. *Vet Pathol* 2003; 40: 481-95.
 37. Samali A, Zhivotovsky B, Jones D, Nagata S, Orrenius S. Apoptosis: cell death defined by caspase activation. *Cell Death Differ* 1999; 6: 495-6.
 38. Ott M, Gogvadze V, Orrenius S, Zhivotovsky B. Mitochondria, oxidative stress and cell death. *Apoptosis* 2007; 12: 913-22.
 39. Rasola A, Bernardi P. The mitochondrial permeability transition pore and its involvement in cell death and in disease pathogenesis. *Apoptosis* 2007; 12: 815-33.
 40. Majno G, Joris I. Apoptosis, oncosis, and necrosis. An overview of cell death. *Am J Pathol* 1995; 146: 3-15.
 41. Zwierzchowski TJ, Stasikowska-Kanicka O, Danilewicz M, Fabiś J. Assessment of apoptosis and MMP-1, MMP-3 and TIMP-2 expression in tibial hyaline cartilage after viable medial meniscus transplantation in the rabbit. *Arch Med Sci* 2012; 8: 1108-14.
 42. Feng W, Li L, Xu X, Jiao Y, Du W. Up-regulation of the long non-coding RNA RMRP contributes to glioma progression and promotes glioma cell proliferation and invasion. *Arch Med Sci* 2017; 13: 1315-21.
 43. Miyashita T, Krajewski S, Krajewska M, et al. Tumor suppressor p53 is a regulator of bcl-2 and bax gene expression in vitro and in vivo. *Oncogene* 1994; 9: 1799-805.
 44. Hsu SY, Kaipia A, McGee E, Lomeli M, Hsueh AJ. Bok is a pro-apoptotic Bcl-2 protein with restricted expression in reproductive tissues and heterodimerizes with selective anti-apoptotic Bcl-2 family members. *Proc Natl Acad Sci USA* 1997; 94: 12401-6.
 45. Ellulu MS, Patimah I, Khaza'ai H, Rahmat A, Abed Y. Obesity and inflammation: the linking mechanism and the complications. *Arch Med Sci* 2017; 13: 851-63.
 46. Hockenbery DM, Oltvai ZN, Yin XM, Millman CL, Korsmeyer SJ. Bcl-2 functions in an antioxidant pathway to prevent apoptosis. *Cell* 1993; 75: 241-51.
 47. Boise LH, González-García M, Postema CE, et al. Bcl-x, a bcl-2-related gene that functions as a dominant regulator of apoptotic cell death. *Cell* 1993; 74: 597-608.
 48. Mattson MP, Kroemer G. Mitochondria in cell death: novel targets for neuroprotection and cardioprotection. *Trends Mol Med* 2003; 9: 196-205.
 49. Kannan K, Jain SK. Oxidative stress and apoptosis. *Pathophysiology* 2000; 7: 153-63.
 50. Demedts IK, Demoor T, Bracke KR, Joos GF, Brusselle GG. Role of apoptosis in the pathogenesis of COPD and pulmonary emphysema. *Respir Res* 2006; 7: 53.
 51. Zhang C, Yu H, Shen Y, Ni X, Shen S, Das UN. Polyunsaturated fatty acids trigger apoptosis of colon cancer cells through a mitochondrial pathway. *Arch Med Sci* 2015; 11: 1081-94.
 52. Abogresha NM, Greish SM, Abdelaziz EZ, Khalil WF. Remote effect of kidney ischemia-reperfusion injury on pancreas: role of oxidative stress and mitochondrial apoptosis. *Arch Med Sci* 2016; 12: 252-62.
 53. Kutwin M, Sawosz E, Jaworski S, et al. Investigation of platinum nanoparticle properties against U87 glioblastoma multiforme. *Arch Med Sci* 2017; 13: 1322-34.
 54. Niedzielski JK, Oszukowska E, Słowikowska-Hilczner J. Undescended testis – current trends and guidelines: a review of the literature. *Arch Med Sci* 2016; 12: 667-77.
 55. Sarkar SA, Kutlu B, Velmurugan K, et al. Cytokine-mediated induction of anti-apoptotic genes that are linked to nuclear factor kappa-B (NF- κ B) signalling in human islets and in a mouse beta cell line. *Diabetologia* 2009; 52: 1092-101.
 56. Chiorazzi N. Chronic lymphocytic leukemia. *Indian J Hematol Blood Transfus* 2013; 29: 1-10.
 57. Sarkar SA, Kutlu B, Velmurugan K, et al. Cytokine-mediated induction of anti-apoptotic genes that are linked to nuclear factor kappa-B (NF- κ B) signalling in human islets and in a mouse beta cell line. *Diabetologia* 2009; 52: 1092-101.
 58. Eder P, Łykowska-Szuber L, Kreła-Każmierczak I, et al. Disturbances in apoptosis of lamina propria lymphocytes in Crohn's disease. *Arch Med Sci* 2015; 11: 1279-85.
 59. Peters JM, Hollingshead HE, Gonzalez FJ. Role of peroxisome-proliferator-activated receptor β/δ (PPAR β/δ) in gastrointestinal tract function and disease. *Clin Sci (Lond)* 2008; 115: 107-27.
 60. Shah DH, Zhou X, Kim HY, Call DR, Guard J. Transposon mutagenesis of *Salmonella enterica* serovar enteritidis identifies genes that contribute to invasiveness in human and chicken cells and survival in egg albumen. *Infection and Immunity* 2012; 80: 4203-15.
 61. Bukulmez O. Endometriosis, inflammation and nuclear receptors. *J Endometriosis* 2012; 4: 129-46.